Received: 21 May 2020 | Revised: 24 August 2020 | Accepted: 30 August 2020
DOI: 10.1002/app.49984

ARTICLE

Applied Polymer SCIENCE WILEY

Comparative study on the electrical, thermal, and mechanical properties of multiwalled carbon nanotubes filled polypropylene and polyamide 6 micromoldings

Junqi Mei[1] | Xue Lei[1] | Mei Liang[1] | Hang Wu[2] | Shengtai Zhou[1] | Huawei Zou[1] | Yang Chen[1]

[1]The State Key Laboratory of Polymer Materials Engineering, Polymer Research Institute of Sichuan University, Chengdu, China

[2]Beijing Special Vehicle Institute, Beijing, China

Correspondence
Shengtai Zhou and Huawei Zou, The State Key Laboratory of Polymer Materials Engineering, Polymer Research Institute of Sichuan University, Chengdu 610065, China.
Email: qduzst@163.com (S.Z.) and hwzou@163.com (H.Z)

Funding information
Sichuan University, Grant/Award Number: C2019105151; The Fundamental Research Funds for the Central Universities

Abstract

In this work, a series of carbon nanotubes filled polypropylene (PP/CNT) and polyamide 6 (PA6/CNT) composites were prepared by melt blending and subsequently molded by compression molding and microinjection molding (μIM), respectively. Electrical conductivity results indicate that the percolation threshold of corresponding microparts shifted to higher filler concentrations when compared with that of compression molded counterparts, suggesting the prevailing shearing conditions in μIM is unfavorable for the construction of conductive pathways. In addition, Raman spectral analysis shows that there is a preferential alignment of CNTs along the flow direction of microparts. Thermal properties of both melt blended samples and subsequent microparts were evaluated using differential scanning calorimetry and thermogravimetric analysis. The mechanical properties of subsequent microparts are greatly affected by filler concentration, which might be related to the structural change that induced by the state of dispersion of CNTs.

KEYWORDS
conducting polymers, morphology, molding

1 | INTRODUCTION

Recently, microproducts have drawn a growing interest in the fields of optical, biomedical, electronics and microelectromechanical systems (MEMS) among others[1] thanks to the rapid development of science and technology. Microinjection molding (μIM) is an emerging technique to fabricate polymeric micro-components to address the aforementioned needs. One of the most noticeable differences between μIM and traditional injection molding process is in that either the size or the weight of microproducts is particularly small.[2] As a result, extreme shearing and cooling effects coexist in μIM. In this scenario, higher molding temperatures, injection velocities, as well as injection pressures are employed to ensure complete filling of mold cavities in μIM,[3] which will exert a great impact on the properties of microproducts. Previous studies have been mainly focused on μIM of unfilled thermoplastics,[4] however, the preparation of multi-functional polymeric microparts can only be accommodated by molding polymer composites with functional fillers.

Traditionally, the addition of highly conductive fillers into polymer matrices is considered as an effective method to improve overall thermal and electrical conductivities. Although both metallic fillers and carbonaceous

Junqi Mei and Xue Lei contribute equally to this work.

 © 2020 Wiley Periodicals LLC

fillers are commonly used as functional additives, the carbon-based fillers outperform metallic ones due to their excellent resistance to oxidative conditions and low density.[5] Carbon nanotubes (CNTs) which were firstly discovered by Sumio Iijima[6] have sparked a growing interest from both the industrial engineers and scientists due to their high aspect ratio and exceptional mechanical properties. Basically, the tensile strength of CNTs is nearly 11–66 GPa, which is about 100 times higher than that of steel[7–9] while their Young modulus can reach as high as 1 TPa.[10,11] Therefore, CNTs are widely adopted as reinforcing fillers to enhance the mechanical properties of either metallic or polymeric materials.[12–14] Besides, CNTs are typical of very high thermal and electrical conductivities. Dai et al. reported that the electrical resistivity of catalytic MWCNTs ranges from 8×10^{-6} to 20×10^{-6} Ω m.[15] The reported thermal conductivity of CNTs falls in a range of 2000 ∼ 6000 W/mK as per Han and Fina.[16] Under such circumstances, CNTs are often adopted as functional additives to improve the electrical and thermal conductivities of polymer matrices.[17] Other factors that affect the properties of CNT-containing polymer composites include aspect ratio, filler concentration, and the dispersibility of CNTs, the interfacial interaction between host polymers and CNTs as well as the involved processing parameters.[18–20]

As mentioned previously, μIM features very high shearing and cooling effects. The added fillers would experience a certain degree of alignment along melt flow direction, owing to the influence of prevailing shear force fields that induced by advancing polymer melts.[21] The preferred orientation of CNTs can impede the random formation of conductive pathways, thereby impairing electrical conductivity. For example, Ferreira et al.[22] found that the alignment of CNT could disrupt the conductive network, thereby leading to a decrease of electrical conductivity. In addition, Eken et al.[23] reported that CNTs are favored to align along melt flow direction when subject to high shear fields whereas they may reaggregate upon the cession of shearing effect. Similar results were reported by Alig et al..[24] In addition to the favored alignment of CNTs under the intensive shearing effect in μIM, CNTs can achieve a relatively better distribution in host matrix[25] and experience a possible length reduction[26,27] due to the involved severe shearing effect.

Aside from the influence of processing parameters,[28,29] the state of the distribution of CNT largely lies in its interaction with the host polymer matrix. Polyamide 6 (PA6), as a typical type of engineering polymers, is widely employed in all aspects of our daily life. PA6 is a polar and semicrystalline polymer due to the presence of amide groups in chain backbones. In this scenario, CNTs are expected to have a better distribution in PA6 thanks to the enhanced interaction between CNTs and polymer chains. Polypropylene (PP), as a type of semicrystalline commodity polymers, has also been widely used in our daily life. Unlike PA6, the repeating unit of PP is –(CH_3)CH-CH_2- which is nonpolar. Thus, CNTs are primarily distributed in the amorphous region of PP since the dispersion of CNTs within PP crystallites is not thermodynamically favored.[28] As a result, the state of distribution of CNT in PP will differ greatly from that in PA6. Therefore, the electrical, mechanical, and thermal properties of corresponding CNT-containing microparts are of great difference.

In this current study, both PA6 and PP are employed as model matrices and CNT is adopted as the functional filler. The difference in interfacial interactions between both polymers and CNTs is given in the Supporting Information. The big disparity in the calculated surface tension between both polymer/CNT pairs suggests that the state of filler distribution in corresponding host polymers is different, which determines the properties of final moldings. In the present work, no coupling agent or compatibilizer was incorporated even though the interfacial interaction between PP and CNTs is quite poor. In this scenario, the influence of interfacial interactions between host polymers and CNTs on the properties of molded samples will be detailed. In addition, compression molding (CM) which features negligible shearing effects[30] was employed as a comparison to assess the influence of prevailing thermomechanical history in both processing techniques (i.e. CM and μIM) on the properties of subsequent moldings.

2 | EXPERIMENTAL

2.1 | Materials

PP under the tradename of 1034E5 was obtained from ExxonMobil™ Chemical Company. PA6 under the tradename of Ultramid® B3S was purchased from BASF. The multi-walled CNT under the tradename of TNIM2 was supplied by Times Nano (Chengdu, China). According to supplier, the CNT (with a length in the range of 30–50 μm) was fabricated by chemical vapor deposition method. The outer and inner diameters of CNT are 8–15 and 3–6 nm, respectively.

2.2 | Preparation of CNT-containing microparts

Prior to blending, both PA6 and PP pellets were dried at 80°C for 10 h under vacuum. Then, a series of polymer composites with filler contents of 0.5, 1, 2, 3, 5, 7 and 10 vol% were obtained using a Brabender mixer.

© RightsPlatform

For PP-based composites, experiments were conducted at 190°C and 30 rpm for 10 min while the PA6/CNT composites were prepared at 240°C and 30 rpm for 10 min. Afterwards, both blends were pulverized to generate small particles for subsequent CM and μIM. Figure 1 displays 3D view of a micropart. The microparts have a thickness × width × length of $0.3 \times 2.0 \times 18.0$ mm^3. For PP/CNT microparts, μIM experiments were conducted at a melt temperature of 200°C and a mold temperature of 80°C. For PA6/CNT microparts, μIM experiments were performed at a melt temperature of 260°C and a mold temperature of 80 °C. In both cases, injection velocity and clamping pressure were 300 mm/s and 100 MPa, respectively. CM of both PP/CNT and PA6/CNT composites was carried out at 190°C for 10 min and at 240°C for 10 min, respectively, both under the pressure of 10 MPa.

2.3 | Characterization

2.3.1 | Electrical conductivity measurements

The electrical conductivity for both compression molded samples and corresponding microparts was determined using two-probe method with a Keysight 34401A 6½ Digit Multimeter (Agilent Technologies Inc., USA).

2.3.2 | Morphology

The morphology for both compression molded and corresponding microparts was observed using scanning electron microscopy (SEM; Thermoscientific Apreo S, Oxford Instruments). Samples for observations were fractured in liquid nitrogen and gold-sputtered to enhance image resolution.

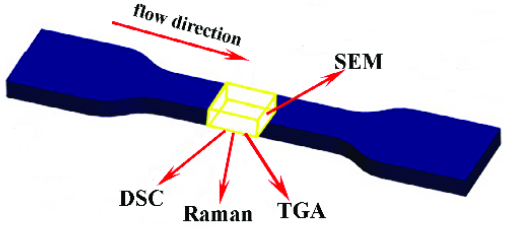

FIGURE 1 Schematic drawing of the sampling methods for DSC, TGA, SEM, and Raman analyses. DSC, differential scanning calorimeter; SEM, scanning electron microscopy, scanning electron microscopy; TGA, thermogravimetric analysis [Color figure can be viewed at wileyonlinelibrary.com]

2.3.3 | Rheology

The viscoelastic behavior of compression molded samples was characterized using a dynamic rheometer (Bohlin Gemini 2000, Malvern) in the melt state. All samples were studied under a constant-strain mode. In order to keep the response in linear viscoelastic region, the applied strain was set at 1%. All samples were prepared in a parallel-plate form with a diameter of 25 mm and thickness of 1 mm, and the rheological tests were performed with a gap distance of 1 mm under nitrogen. All samples were tested in a frequency sweep range from 0.01 to 100 Hz. The testing temperatures for both PP- and PA6-based samples are 190°C and 240°C, respectively.

2.3.4 | Differential scanning calorimetry

The thermal behavior of both compression molded composites and corresponding microparts were traced by a differential scanning calorimeter (DSC-204, Netzsch, Germany). All experiments were conducted under nitrogen with a gas flow rate of 50 ml/min. The measurement procedure for all samples is described below: taking PP-based samples for example, the sample was initially heated from 30 to 200°C at 10°C /min; then, it was held at 200°C for 3 min to erase thermal history; afterwards, the sample was cooled to 30°C at 10°C /min. Again, it was held at 30°C for another 3 min then heated to 200°C at 10°C /min. Characterization for PA6/CNT samples followed the same produce except that PA6/CNT counterparts were heated to 260°C. Both the melting temperature and crystallization temperature were obtained from the heating and cooling cycles, respectively. The crystallinity (χ_c) obtained from both heating cycles was calculated as per Equation 1.

$$\chi_c = (\Delta H_m)/\left(\Delta H^{calc}\right) \times 100\% (1).$$

where ΔH_m is the observed melting enthalpy of either PP or PA6, and ΔH^{calc} is the product of melting enthalpy for 100% crystalline polymer and its weight fraction in CNT-containing polymer composites. The melting enthalpies of 100% crystalline polymer for both PP and PA6 are 207[31] and 230[32] J/g, respectively.

2.3.5 | Thermogravimetric analysis

Thermogravimetric analysis (TGA) was performed using a thermogravimetric analyzer (TG 209F1, NETZSCH, Germany) to study the thermal stability under nitrogen

© RightsPlatform

with a flow rate of 60 ml/min. To study the influence of thermomechanical history on the thermal stability of CNT-containing polymer composites, a comparison between both compression molded composites and the Middle region of corresponding microparts was conducted. All samples were scanned at 10°C/min and the relative weight loss was recorded from 35 to 800°C.

2.3.6 | Raman spectral analysis

Raman spectra were collected using a ThermoScientific spectrometer which was equipped with a DXRxi Raman imaging microscope. Samples were excited using a 532 nm laser and the spectral range is from 50 to 3400 cm^{-1}. The measurements were carried out on both compression molded composites and the Middle region of corresponding microparts. Three replicates were tested and the average values were adopted.

2.3.7 | Mechanical properties

The mechanical properties of CNT-containing microparts were tested using a universal mechanical tester (Instron 5569, Instron Corporation, UK) with a crosshead speed of 10 mm/min. The gap distance is kept at 10 mm. Five specimens were tested for each measurement.

3 | RESULTS AND DISCUSSION

3.1 | Electrical conductivity

The σ for both pure PP and PA6 cannot be detected, and the σ increases for both polymers with an incremental loading fraction of CNT. Figure 2 shows the σ of both compression molded PP/CNT and PA6/CNT composites as well as their corresponding microparts, as a function of filler content. Figure 2(a) indicates that the σ for both PP/CNT and PA6/CNT composites is enhanced with increasing filler concentration. Moreover, changes of σ is largely dependent on the types of employed polymers. For example, the percolation threshold (p_c) of PP/CNT composites is detected in the vicinity of 1 vol% whereas the p_c is nearly 5 vol% (or more specifically $3 \sim 5$ vol%) for PA6/CNT counterparts. In addition, the values of σ for both compression molded PP/CNT composites and related microparts are invariably higher than their PA6/CNT counterparts, suggesting that CNTs are more easily to form conductive pathways within PP. According to Moud et al.,[33] the CNTs are poorly distributed in PP, and the presence of small size CNT agglomerates makes it easier to form conductive pathways, thereby leading to the enhancement of σ for PP/CNT composites. But, the well dispersed CNTs which is due to better interfacial interactions between PA6 and CNTs are unlikely to form a number of small size agglomerates, which is unfavorable for the construction of conductive pathways. The polar amide groups on PA6 chain backbones have a great affinity to CNTs, which facilitates the dispersion of CNTs.[34] In this scenario, the presence of a layer of PA6 matrix surrounding CNTs impairs the enhancement of σ.[27]

Figure 2(b) shows that the σ cannot be detected for PP/CNT and PA6/CNT microparts when the filler content is less than 5 vol% and 7 vol%, respectively, indicating that CNTs are unlikely to form 3D conductive pathways although the filler concentrations are relatively high, under the conditions of μIM. Abbasi et al.[30] reported that the prevailing shear rates in μIM are a few orders of magnitude higher than those encountered in

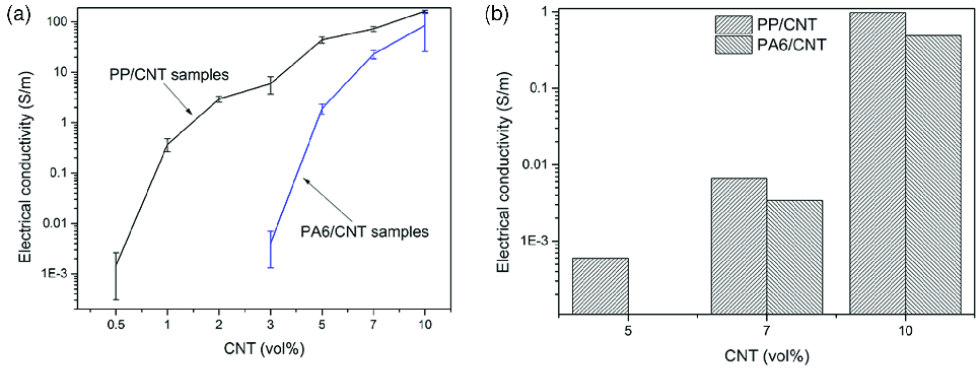

FIGURE 2 The volume electrical conductivity (σ) of both (a) compression molded samples and (b) microinjection molded samples, as a function of CNT content [Color figure can be viewed at wileyonlinelibrary.com]

© RightsPlatform

CM. Under such circumstances, CNTs are preferentially aligned along the melt flow direction of the microparts,[35] thereby impairing random construction of conductive pathways. Aside from severe shearing conditions, μIM is characteristic of fast cooling.[36,37] It is noted that the mold cavities can be completely filled within a few milliseconds and polymer melts can be "frozen" instantly when they come into contact with the cold mold wall.[3,38] In this scenario, the "frozen" polymer chains and CNTs would be typically aligned along the flow direction and they are unlikely to return to their original random distribution state.[39] As a result, the σ for microparts is invariably lower than that of compression molded counterparts.

3.2 | Morphology

The morphology of cryo-fractured surface of both compression molded and microinjection molded PP/CNT composites is given in Figure 3. Results reveal that CNT agglomerates are present in both compression molded

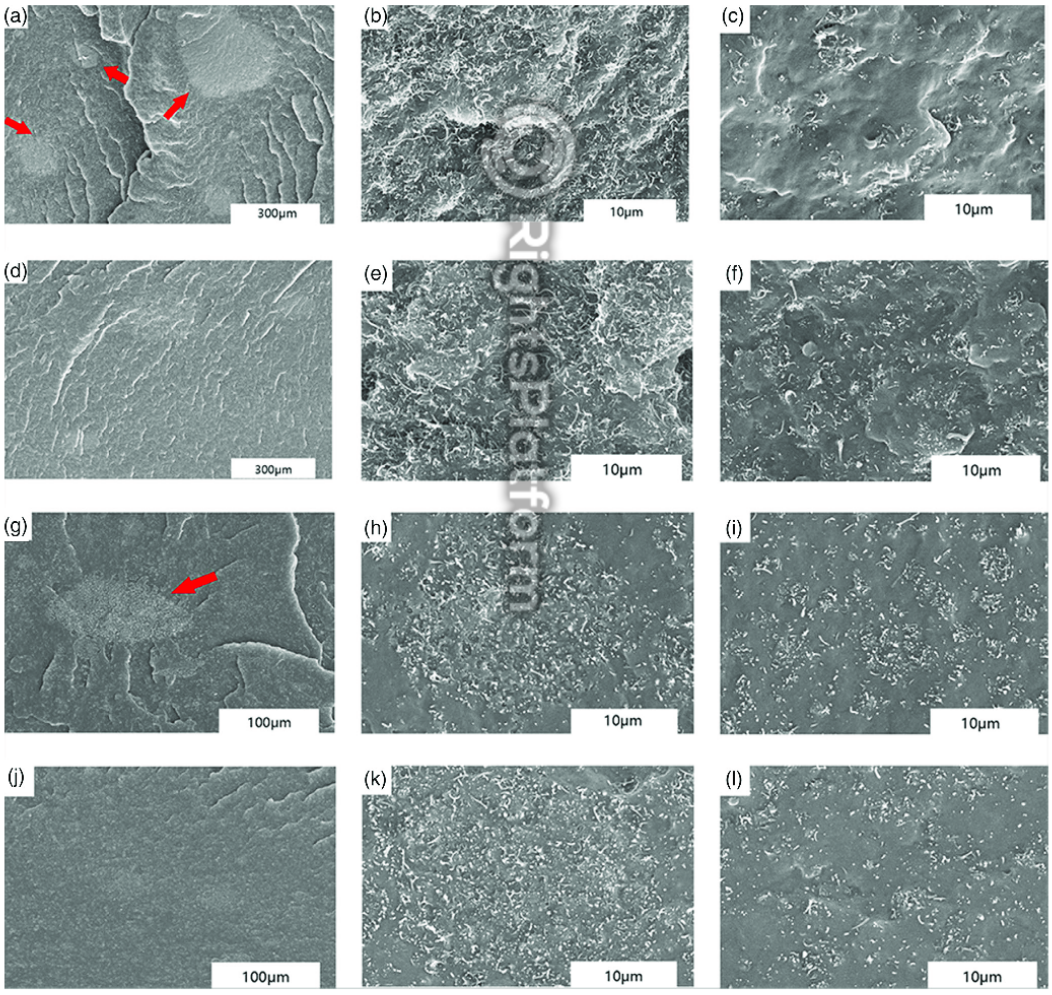

FIGURE 3 Images of (a-c) compression molded PP/CNT 3 vol% composites; (g-i) PP/CNT 3 vol% microparts; (d-f) compression molded PP/CNT 5 vol% composites and (j-l) PP/CNT 5 vol% microparts. PP/CNT, carbon nanotubes filled polypropylene [Color figure can be viewed at wileyonlinelibrary.com]

PP/CNT composites and microinjection molded counterparts. As can be seen from Figure 3(a), the size of CNT agglomerates can be as big as a few hundred microns, as indicated by the red arrows. Figure 3(b) was observed from areas with large size CNT agglomerates (as pointed out by red arrows) and it shows that CNTs are heavily entangled with each other to form intact conductive pathways. Figure 3(c) was taken from regions outside of large CNT agglomerates and it clearly shows that although the distribution of CNTs is not as compact as that observed in Figure 3(b), they can still form conductive pathways via physical connection among individual fillers.

However, when the filler concentration is increased to 5 vol%, the size of CNT agglomerates is slightly reduced when compared with that of PP/CNT 3 vol% counterparts, as shown in Figure 3(g). This can be attributed to the fact that the viscosity of polymer melts can be significantly increased with increasing filler content (as verified by rheology analysis), especially for CNT-filled polymer composites.[5] In this scenario, the rupture mechanism governs when a higher viscosity polymer composite was involved in terms of dispersing CNTs as per Alig et al.[24] Therefore, large size CNT agglomerates could be ruptured by the applied shear force during melt compounding process. Figure 3(e),(f) were taken from the CNT agglomerates and regions outside of CNT agglomerates, respectively. In both cases, intact conductive network was constructed by CNTs, which is crucial to the enhancement of σ for corresponding polymer composites.

In addition, the distribution of CNTs is improved when the composites were subjected to μIM. Figure 3(g), (j) show that the size of CNT agglomerates is significantly reduced when compared with their compression molded counterparts. This is undoubtedly related to the effect of prevailing shear rates in μIM. According to Jiang et al.,[40] shear rates as high as 10^6 /s are not rare in μIM. In this scenario, spherical CNT agglomerate would deform under the intensive shearing conditions. Moreover, Li and Shimizu[25] have reported that CNTs can achieve a relatively better distribution when they were processed under high shear conditions. Similar results were reported in previous studies.[27,28] However, a better distribution of CNTs may not contribute to the enhancement of σ since well-constructed conductive network that formed by CNTs can be destructed under the combined influence of intensive shearing and fast cooling effects in μIM[39] As a result, the σ of PP/CNT microparts is lower than that of compression molded counterparts.

Figure 4 displays SEM images of both compression molded and microinjection molded PA6/CNT composites. Unlike PP/CNT composites, the size of CNT agglomerates is greatly reduced in PA6. Also CNTs have a relatively uniform distribution in PA6 than that in PP, which can be attributed to the difference of interfacial affinity between CNTs and host matrices.[35] PA6 is a polar, semicrystalline polymer, which has a strong affinity with CNT, thereby favoring the distribution of fillers.[27] PP is a nonpolar, semicrystalline polymer which has poor interfacial interaction with CNT. Additionally, the presence of crystallites within PP would force CNTs to mainly disperse in amorphous region which, to a certain degree, results in the formation of CNT agglomerates.[35,39] Similar to PP/CNT composites, the size of CNT agglomerates in PA6/CNT composites is greatly reduced with increasing filler content. For example, no visible CNT clusters can be observed in PA6/CNT 3 vol% microparts [see Figure 4(d)] when compared with that in compression molded counterparts [Figure 4(a)]. Additionally, the distribution of CNTs in PA6/CNT microparts was also greatly improved due to the prevailing severe shearing conditions. Previous study[27] have shown that a length reduction of CNT might have occurred in μIM, which has a detrimental effect on the enhancement of σ for subsequent moldings. Although it seems that CNTs have a better distribution in PA6/CNT 5 vol% microparts [Figure 4(j-l)], the σ of PA6/CNT microparts is hardly detected until the filler concentration reaches 7 vol%.

3.3 | Rheology

The viscoelastic properties of both the PP/CNT and PA6/CNT composites as a function of frequency at various filler content are displayed in Figure 5. Figure 5(a), (b) show that the values of both elastic modulus (G′) and viscous modulus (G″) increase with increasing CNT concentration. Figure 5(a),(b) indicate that both G′ and G″ are sensitive to evaluate the rheological behavior of samples depending on the structural changes in the composites, especially at low frequency region. Starting from 2 vol% CNT, a plateau tends to be found at low frequency regions in both the G′ and G″. In addition, a pronounced shear thinning behavior is noticeable in the behavior of complex viscosity (η*) when the concentration of CNT is at least 2 vol%, as displayed in Figure 5(c). This relation is a well-known phenomenon for polymer composites, which indicates a physical network formation by inorganic fillers.[32,41] Thus, the rheological percolation can be determined using rheological data as per Pötschke et al.[42] Above 2 vol% CNT, the rheological behavior changes from a viscous fluid to an elastic solid, indicating that the formation of intact conductive pathways formed by CNTs. This result is consistent with the electrical conductivity measurements where a remarkable increase of σ

© RightsPlatform

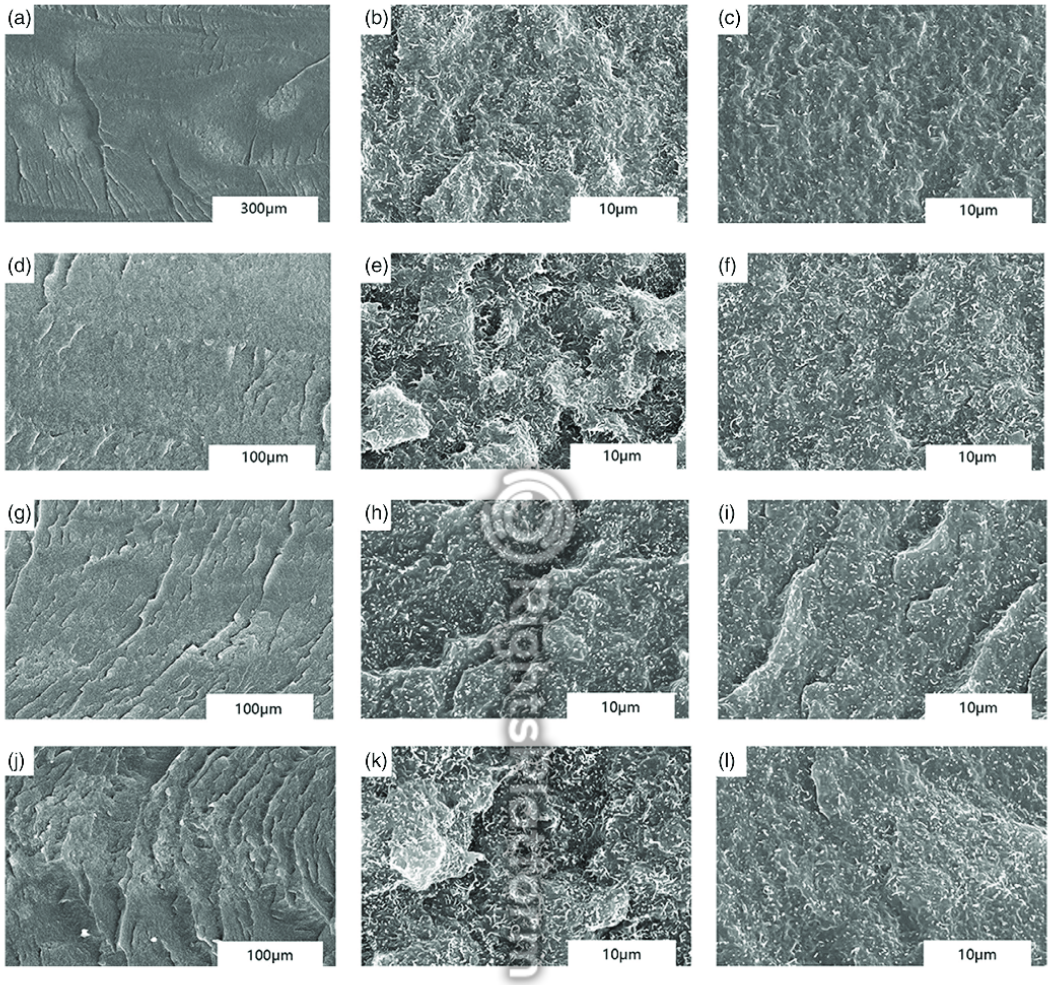

FIGURE 4 Images of (a-c) compression molded PA6/CNT 3 vol% composites; (g-i) PA6/CNT 3 vol% microparts; (d-f) compression molded PA6/CNT 5 vol% composites and (j-l) PA6/CNT 5 vol% microparts. PA6, polyamide 6; PP/CNT, carbon nanotubes filled polypropylene

was observed in the vicinity of the rheological percolation region (around 2 vol%), as depicted in Figure 2(a).

Unlike PP/CNT system, the viscoelastic behavior (i.e. G', G'' and η^*) of PA6/CNT 0.5 vol% composite does not vary greatly when compared with that of pure PA6. However, they deviate from those of pure PA6 with further increasing filler concentration, suggesting that well dispersed CNTs in PA6 has an obvious reinforcement effect. Although a plateau is detected when the filler concentration is around 3 vol%, the σ of PA6/CNT composites still falls out of the lower limit for the measurement range of the Agilent electrometer. Thus, a higher filler concentration ($\geq$ 3 vol%) is required to attain sufficient conductive pathways within PA6, as reflected in Figure 2(b).

3.4 | Melting and crystallization properties

Figure 6 exhibits the melting and crystallization behavior of melt blended PP/CNT composites and subsequent PP/CNT microparts. Typical thermal analysis data that obtained from these diagrams are listed in Table 1.

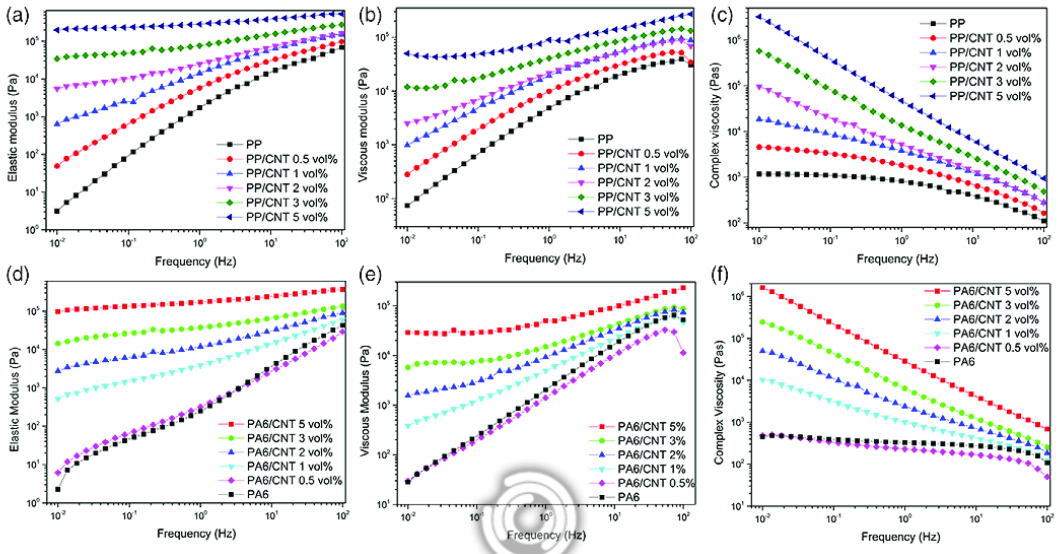

FIGURE 5 The viscoelastic behavior of both PP/CNT (temperature: 200°C) and PA6/CNT composites (temperature: 260°C) as a function of frequency at various filler content. All samples were prepared by compression molding. PA6, polyamide 6; PP/CNT, carbon nanotubes filled polypropylene [Color figure can be viewed at wileyonlinelibrary.com]

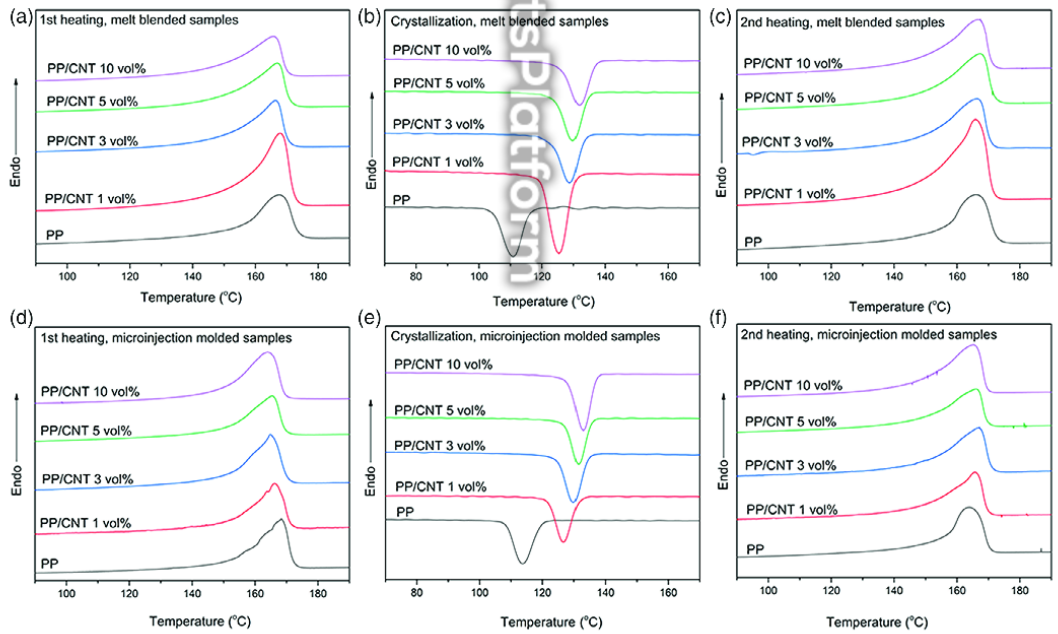

FIGURE 6 The melting and crystallization behavior of both compression molded and microinjection molded PP/CNT composites. PP/CNT, carbon nanotubes filled polypropylene [Color figure can be viewed at wileyonlinelibrary.com]

TABLE 1 Typical thermal analysis data obtained from DSC tests for PP/CNT composites prepared by different methods

Sample	Vol%	T_m (°C)		T_c (°C)	χ_c (%)	
		Cycle 1	Cycle 3	Cycle 2	Cycle 1	Cycle 3
Melt blended	0	167.7	165.9	110.0	26.54	26.19
	1	167.3	165.5	126.3	45.74	47.77
	3	167.7	167.9	128.6	49.29	48.88
	5	166.9	167.3	129.7	31.23	32.92
	10	165.7	167.5	131.8	31.86	34.62
μIM	0	168.4	163.8	113.8	30.17	30.25
	1	166.2	165.7	126.7	30.46	33.22
	3	164.8	167.2	129.8	35.57	39.78
	5	165.3	166.0	131.4	31.21	35.10
	10	163.9	163.9	133.0	42.12	48.76

Abbreviations: DSC, differential scanning calorimeter; PP/CNT, carbon nanotubes filled polypropylene; μIM, microinjection molding.

Figure 6(a) shows that the melting temperature (T_m) of PP/CNT composites changes slightly with an incremental loading content of CNT. However, T_m of subsequent PP/CNT microparts decreases with increasing filler concentration. In addition, the T_m of pure PP micropart is 0.7°C higher than that of melt blended PP counterpart, which might be related to shear induced crystallization of polymer chains, under the severe shearing conditions in μIM. Microparts also experience fast cooling due to their large surface area to volume ratio. In this scenario, the oriented polymer chains can be 'frozen' instantly, which is advantageous to the enhancement of χ_c for PP microparts, as given in Table 1. Meanwhile, the presence of CNTs may hinder, to a certain degree, the alignment of polymer chains, which results in a slight reduction of T_m for PP/CNT microparts.

Moreover, the crystallization temperature (T_c) increases with an incremental loading content of CNT, as depicted in Figure 6(b). This is related to the heterogeneous nucleation effect of CNT.[43] The above also indicates that the crystallization process of PP was associated with the number of crystallization sites that provided by CNT, which is consistent with the results reported by Kazemi et al..[44] Table 1 shows that the addition of CNT greatly affects the χ_c of PP, irrespective of heating cycles. For example, increased χ_c is observed for PP/CNT composites and corresponding microparts with the addition of up to 3 vol% CNT, which suggests that CNTs offer crystallization sites for PP chains, thereby leading to an increase of χ_c. However, further increasing CNT concentrations leads to a reduction of χ_c for both PP/CNT composites and corresponding microparts. In this scenario, the existence of a large number of CNTs would hinder the formation of stable crystallites due to limited space and confinement effect that imposed on polymer chains by CNT.[45] In general, the χ_c for PP/CNT microparts that obtained from the second heating cycle (i.e. Cycle 3) is higher than that obtained from the first heating cycle (Cycle 1), suggesting that the thermomechanical history significantly affects the thermal properties of PP/CNT composites.

Figure 7 demonstrates the melting and crystallization behavior of PA6/CNT composites and corresponding microparts. Typical thermal analysis data that obtained from these diagrams are listed in Table 2. Table 2 shows that there is a reduction of T_m with the incorporation of CNT, and the T_m of PA6/CNT microparts is slightly lower than that of corresponding composites. This suggests that the presence of CNT has a hindrance effect on the formation of stable crystallites, and the extreme shearing and cooling effects are also unfavorable for the formation of well-defined crystals, thereby leading to a reduction of T_m.

Moreover, the crystallization process is greatly affected with the addition of CNT. Only a single crystallization peak (T_{c1}) is detected in the vicinity of 170°C for pure PA6 matrix and around 190°C for pure PA6 microparts. The increase of T_c for pure PA6 microparts suggests a flow induced crystallization that induced by the prevailing shearing rates. In addition, T_c increases slightly with the content of CNT, as displayed in Figure 7 (b),(e) as well as Table 2. This phenomenon could be attributed to the heterogeneous nucleation effect that induced by CNTs. Furthermore, a second crystallization temperature (T_{c2}) is typically observed at higher temperatures for CNT-containing PA6 composites, and its position gradually shifted to higher temperature regions with an increasing content of CNT, suggesting that the

© RightsPlatform

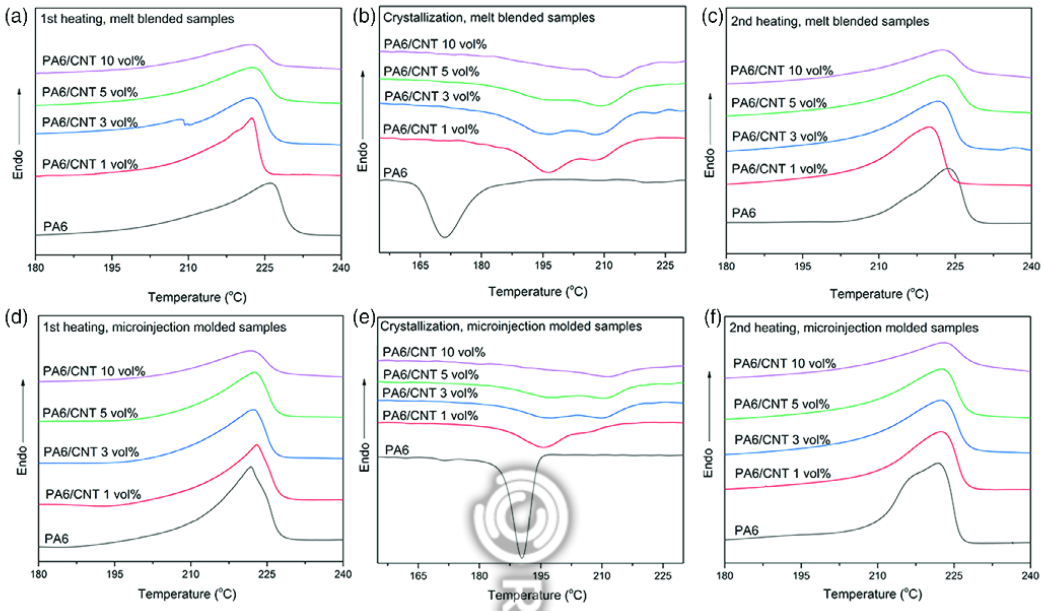

FIGURE 7 The melting and crystallization behavior of both compression molded and microinjection molded PA6/CNT composites. CNT, carbon nanotubes filled; PA6, polyamide 6 [Color figure can be viewed at wileyonlinelibrary.com]

TABLE 2 Typical thermal analysis data obtained from DSC tests for PA6/CNT composites prepared by different methods

		T_m (°C)		T_c (°C)		χ_c (%)	
Sample	**Vol%**	**Cycle 1**	**Cycle 3**	T_{c1}	T_{c2}	**Cycle 1**	**Cycle 3**
Melt blended	0	226.1	223.8	171.1	–	34.13	21.15
	1	223.5	221.0	197.2	207.6	26.72	30.53
	3	223.4	222.9	198.2	208.6	31.71	27.24
	5	222.9	222.8	202.6	209.4	26.72	26.69
	10	222.2	222.6	–	213.5	26.17	27.80
μIM	0	221.8	221.8	190.6	–	34.07	32.03
	1	223.1	222.6	195.4	–	24.92	23.39
	3	222.6	222.6	197.9	209.7	23.82	28.11
	5	222.4	222.6	197.8	210.9	22.97	24.95
	10	221.9	223.5	–	212.2	20.99	23.82

Abbreviations: DSC, differential scanning calorimeter; PA6, polyamide 6; μIM, microinjection molding.

appearance of T_{c2} in PA6 is related to the presence of CNT. Similar observations were reported by Logakis et al.[46] In literature,[27,46] two possible mechanisms have been proposed to explain the appearance of double crystallization peak in PA6/CNT composites, which are the formation of two different types of crystals (i.e. the transcrystalline structure and spherical structure) or two-step crystallization process due to the presence of one-dimensional filler, i.e. CNT. Unlike PP/CNT composites, the χ_c of PA6/CNT composites and corresponding microparts decrease with increasing filler content. This may be ascribed to the well distribution of CNT in the host matrix which hinders the formation of stable crystals during processing.